Void-nanograting transition by ultrashort laser pulse irradiation in silica glass

Ye Dai,[1, 2, *] Aabid Patel,[2] Juan Song,[3] Martynas Beresna,[2] and Peter G. Kazansky[2]

[1]*Department of Physics, Shanghai University, Shanghai 200444, China*
[2]*Optoelectronics Research Centre, University of Southampton, Southampton SO17 1BJ, United Kingdom*
[3]*School of Material Science and Engineering, Jiangsu University, Zhenjiang 212013, China*
[*]*yedai@shu.edu.cn*

Abstract: The structural evolution from void modification to self-assembled nanogratings in fused silica is observed for moderate (NA > 0.4) focusing conditions. Void formation, appears before the geometrical focus after the initial few pulses and after subsequent irradiation, nanogratings gradually occur at the top of the induced structures. Nonlinear Schrödinger equation based simulations are conducted to simulate the laser fluence, intensity and electron density in the regions of modification. Comparing the experiment with simulations, the voids form due to cavitation in the regions where electron density exceeds 10^{20} cm^{-3} but is below critical. In this scenario, the energy absorption is insufficient to reach the critical electron density that was once assumed to occur in the regime of void formation and nanogratings, shedding light on the potential formation mechanism of nanogratings.

OCIS codes: (140.3390) Laser materials processing; (140.3440) Laser-induced breakdown; (050.6624) Subwavelength structures; (320.7120) Ultrafast phenomena.

References and links

1. R. Gattass, E. Mazur, "Femtosecond laser micromachining in transparent materials," Nat. Photonics **2**(4), 219–225 (2008).
2. K. Sugioka, Y. Cheng, "Ultrafast lasers—reliable tools for advanced materials processing," Light Sci. Appl. **3**, e149 (2014).
3. J. W. Chan, T. Huser, S. Risbud, and D. M. Krol, "Structural changes in fused silica after exposure to focused femtosecond laser pulses," Opt. Lett. **26**(21), 1726–1728 (2001).
4. A. M. Streltsov, N. F. Borrelli, "Study of femtosecond-laser-written waveguides in glasses," J. Opt. Soc. Am. B **19**(10), 2496-2504 (2002).
5. A. Zoubir, C. Rivero, R. Grodsky, K. Richardson, M. Richardson, T. Cardinal, and M. Couzi, "Laser-induced defects in fused silica by femtosecond IR irradiation," Phys. Rev. B **73**(22), 224117 (2006).
6. V. R. Bhardwaj, P. B. Corkum, D. M. Rayner, C. Hnatovsky, E. Simova, and R. S. Taylor, "Stress in femtosecond-laser-written waveguides in fused silica," Opt. Lett. **29**(12), 1312–1314 (2004).
7. Y. Shimotsuma, P. Kazansky, J. Qiu, and K. Hirao, "Self-organized nanogratings in glass irradiated by ultrashort light pulses," Phys. Rev. Lett. **91**(24), 247405 (2003).
8. V. R. Bhardwaj, E. Simova, P. P. Rajeev, C. Hnatovsky, R. S. Taylor, D. M. Rayner, and P. B. Corkum, "Optically produced arrays of planar nanostructures inside fused silica," Phys. Rev. Lett. **96**(5), 057404 (2006).
9. E. Bricchi, P. G. Kazansky, "Extraordinary stability of anisotropic femtosecond direct-written structures embedded in silica glass," Appl. Phys. Lett. **88**(11), 111119 (2006).
10. D. Du, X. Liu, G. Korn, J. Squier, and G. Mourou, "Laser-induced breakdown from 7 ns to 150 fs by impact ionization in SiO_2 with pulse widths," Appl. Phys. Lett. **64**(23), 3071–3073 (1994).
11. J. H. Marburger, "Self-focusing: theory," Prog. Quantum Electron. **4**(75), 35–110 (1975).
12. E. N. Glezer, E. Mazur, "Ultrafast-laser driven micro-explosions in transparent materials," Appl. Phys. Lett. **71**(7), 882–884 (1997).
13. S. Juodkazis, H. Misawa, T. Hashimoto, E. G. Gamaly, and B. Luther-Davies, "Laser-induced microexplosion confined in a bulk of silica: Formation of nanovoids," Appl. Phys. Lett. **88**(20), 201909 (2006).

14. S. Juodkazis, K. Nishimura, S. Tanaka, H. Misawa, E. G. Gamaly, B. Luther-Davies, L. Hallo, P. Nicolai, and V. T. Tikhonchuk, "Laser-induced microexplosion confined in the bulk of a sapphire crystal: evidence of multimegabar pressures," Phys. Rev. Lett. **96**(16), 166101 (2006).
15. S. Kanehira, J. Si, J. Qiu, K. Fujita, and K. Hirao, "Periodic nanovoid structures via femtosecond laser irradiation," Nano Lett. **5**(8), 1591–1595 (2005).
16. E. Toratani, M. Kamata, and M. Obara, "Self-fabrication of void array in fused silica by femtosecond laser processing," Appl. Phys. Lett. **87**(17), 171103 (2005).
17. C. Mauclair, A. Mermillod-Blondin, S. Landon, N. Huot, A. Rosenfeld, I. V Hertel, E. Audouard, I. Myiamoto, and R. Stoian, "Single-pulse ultrafast laser imprinting of axial dot arrays in bulk glasses," Opt. Lett. **36**(3), 325–327 (2011).
18. H. Y. Sun, J. Song, C. B. Li, J. Xu, X. S. Wang, Y. Cheng, Z. Z. Xu, J. R. Qiu, and T. Q. Jia, "Standing electron plasma wave mechanism of void array formation inside glass by femtosecond laser irradiation," Appl. Phys. A **88**(2), 285–288 (2007).
19. A. Vogel, N. Linz, S. Freidank, and G. Paltauf, "Femtosecond-laser-induced nanocavitation in water: Implications for optical breakdown threshold and cell surgery," Phys. Rev. Lett. **100**(3), 038102 (2008).
20. R. Taylor, C. Hnatovsky, and E. Simova, "Applications of femtosecond laser induced self-organized planar nanocracks inside fused silica glass," Laser Photon. Rev. **2**(1–2), 26–46 (2008).
21. F. Liang, R. Vallée, and S. L. Chin, "Mechanism of nanograting formation on the surface of fused silica," Opt. Express **20**(4), 4389-4396 (2012).
22. S. Richter, F. Jia, M. Heinrich, S. Döring, U. Peschel, A. Tünnermann, and S. Nolte, "The role of self-trapped excitons and defects in the formation of nanogratings in fused silica," Opt. Lett. **37**(4), 482-484 (2012).
23. M. Beresna, M. Gecevičius, P. G. Kazansky, T. Taylor, and A. V. Kavokin, "Exciton mediated self-organization in glass driven by ultrashort light pulses," Appl. Phys. Lett. **101**(5), 053120 (2012).
24. R. Buividas, L. Rosa, R. Sliupas, T. Kudrius, G. Slekys, V. Datsyuk, and S. Juodkazis, "Mechanism of fine ripple formation on surfaces of (semi)transparent materials via a half-wavelength cavity feedback," Nanotechnology **22**(5), 055304 (2011).
25. Y. Liao, W. Pan, Y. Cui, L. Qiao, Y. Bellouard, K. Sugioka, and Y. Cheng, "Formation of in-volume nanogratings with sub-100-nm periods in glass by femtosecond laser irradiation," Opt. Lett. **40**(15), 3623-3626 (2015).
26. Y. Liao, J. Ni, L. Qiao, M. Huang, Y. Bellouard, K. Sugioka, Y. Cheng, "High-fidelity visualization of formation of volume nanogratings in porous glass by femtosecond laser irradiation," Optica **2**(4), 329-334 (2015).
27. A. Rudenko, J. Colombier, and T. E. Itina, "From random inhomogeneities to periodic nanostructures induced in bulk silica by ultrashort laser," Phys. Rev. B **93**(7), 075427 (2016).
28. K. Mishchik, C. D'Amico, P. K. Velpula, C. Mauclair, a. Boukenter, Y. Ouerdane, and R. Stoian, "Ultrafast laser induced electronic and structural modifications in bulk fused silica," J. Appl. Phys. **114**(13), 133502 (2013).
29. L. Sudrie, A. Couairon, M. Franco, B. Lamouroux, B. Prade, S. Tzortzakis, and A. Mysyrowicz, "Femtosecond laser-induced damage and filamentary propagation in fused silica," Phys. Rev. Lett. **89**(18), 186601 (2002).
30. A.-C. Tien, S. Backus, H. Kapteyn, M. Murnane, and G. Mourou, "Short-pulse laser damage in transparent materials as a function of pulse duration," Phys. Rev. Lett. **82**(19), 3883–3886 (1999).
31. M. Lancry, B. Poumellec, J. Canning, K. Cook, J. C. Poulin, and F. Brisset, "Ultrafast nanoporous silica formation driven by femtosecond laser irradiation," Laser Photonics Rev. **7**(6), 953–962 (2013).
32. M. Beresna, M. Gecevičius, M. Lancry, B. Poumellec, and P. G. Kazansky, "Broadband anisotropy of femtosecond laser induced nanogratings in fused silica," Appl. Phys. Lett. **103**(13), 131903(2013).
33. J. Song, X. Wang, X. Hu, Y. Dai, J. Qiu, Y. Cheng, and Z. Xu, "Formation mechanism of self-organized voids in dielectrics induced by tightly focused femtosecond laser pulses," Appl. Phys. Lett. **92**(9), 092904 (2008).
34. A. Okhrimchuk, V. Mezentsev, H. Schmitz, M. Dubov, and I. Bennion, "Cascaded nonlinear absorption of femtosecond laser pulses in dielectrics," Laser Phys. **19**(7), 1415–1422 (2009).
35. Z. Wu, H. Jiang, L. Luo, H. Guo, H. Yang, and Q. Gong, "Multiple foci and a long filament observed with focused femtosecond pulse propagation in fused silica.," Opt. Lett. **27**(6), 448–450 (2002).
36. I. M. Burakov, N. M. Bulgakova, R. Stoian, A. Mermillod-Blondin, E. Audouard, A. Rosenfeld, A. Husakou, and I. V. Hertel, "Spatial distribution of refractive index variations induced in bulk fused silica by single ultrashort and short laser pulses," J. Appl. Phys. **101**(4), 043506 (2007).
37. A. Marcinkevičius, V. Mizeikis, S. Juodkazis, S. Matsuo, and H. Misawa, "Effect of refractive index-mismatch on laser microfabrication in silica glass," Appl. Phys. A **76**(2), 257–260 (2003).
38. P. Török, P. Varga, A. Konkol, and G. R. Booker, "Electromagnetic diffraction of light focused through a planar interface between materials of mismatched refractive indices: an integral representation," J. Opt. Soc. Am. A **12**(2), 325-332 (1995).
39. W. Liu, O. Kosareva, I. S. Golubtsov, A. Iwasaki, A. Becker, V. P. Kandidov, S. L. Chin, "Femtosecond laser pulse filamentation versus optical breakdown in H_2O," Appl. Phys. B **76**(3), 215-229 (2003).

40. A. Couairon, O. G. Kosareva, N. A. Panov, D. E. Shipilo, V. A. Andreeva, V. Jukna, and F. Nesa, "Propagation equation for tight-focusing by a parabolic mirror," Opt. Express **23**(24), 31240-31252 (2015).
41. C. B. Schaffer, A. Brodeur, and E. Mazur, "Laser-induced breakdown and damage in bulk transparent materials induced by tightly focused femtosecond laser pulses," Meas. Sci. Technol. **12**(11), 1784–1794 (2001).
42. E. G. Gamaly, L. Rapp, V. Roppo, S. Juodkazis, and A. V. Rode, "Generation of high energy density by fs-laser-induced confined microexplosion," New J. Phys. **15**(7), 025018 (2013).
43. K. Mishchik, G. Cheng, G. Huo, I. M. Burakov, C. Mauclair, A. Mermillod-Blondin, A. Rosenfeld, Y. Ouerdane, A. Boukenter, O. Parriaux, and R. Stoian, "Nanosize structural modifications with polarization functions in ultrafast laser irradiated bulk fused silica," Opt. Express **18**(20), 24809–24824 (2010).
44. P. P. Saeta, B. B. Greene, "Primary relaxation processes at the band edge of SiO_2," Phys. Rev. Lett. **70**(23), 3588–3591 (1993).
45. D. G. Papazoglou, S. Tzortzakis, "Physical mechanisms of fused silica restructuring and densification after femtosecond laser excitation," Opt. Mater. Express **1**(4), 625–632 (2011).
46. D. G. Papazoglou, I. Zergioti, and S. Tzortzakis, "Plasma strings from ultraviolet laser filaments drive permanent structural modifications in fused silica," Opt. Lett. **32**(14), 2055–2057 (2007).
47. S. Höhm, A. Rosenfeld, J. Krüger, and J. Bonse, "Femtosecond laser-induced periodic surface structures on silica," J. Appl. Phys. **112**(1), 014901 (2012).
48. P. P. Rajeev, M. Gertsvolf, C. Hnatovsky, E. Simova, R. S. Taylor, P. B. Corkum, D. M. Rayner, and V. R. Bhardwaj, "Transient nanoplasmonics inside dielectrics," J. Phys. B. **40**(11), S273–S282 (2007).

1. Introduction

Ultrafast lasers have become a powerful tool in material microprocessing over the years, which has proven to be pivotal in the development of a growing number of fabricated micro/nano-components for a wide range of applications [1]. In particular, as the interaction process between femtosecond laser pulses and condensed matter originates mainly from nonlinear effects, which occur locally near the focus, volumetric space-selective structural modification can be achieved in the bulk of transparent dielectrics [2]. Previous studies have shown that the damage threshold of material depends on multiple parameters of incident laser pulse, such as the wavelength, pulse duration and number. But usually for single femtosecond laser pulse at 800nm, the induced structures in the exposure area mainly depends on the level of the laser intensity and therefore have long been classified qualitatively into three types. (i) Type I is a smooth positive refractive index change observed at a low intensity regime ($<10^{12}$ W/cm^2), which may originate from material densification after structural network reorganization [3,4], formation of agglomerate colour centres or defects [5], or mechanical stress due to pressure wave release [6]. (ii) When the incident intensity exceeds 10^{12} W/cm,^{2} a type II modification (i.e. periodic nanostructure or nanogratings) forms under a multi-pulse exposure condition. This structure consists of alternating nanoplanes, oriented perpendicular to the polarization of light, and exhibits optical birefringence [7–9]. (iii) If the laser intensity exceeds 10^{13} W/cm^2, the density of induced plasma at the focus will continue increasing and potentially reach the critical electron density (1.7×10^{21} cm^{-3} for 800 nm in fused silica) above which the plasma becomes opaque and reflective [10]. The subsequent relaxation, in this case, depends on focusing conditions and pulse number density.

If a single pulse with energy lower than the critical power ($P_{cr} = 3.77\lambda^2 / 8\pi n_0 n_2$ [11]) is tightly focused at a shallow depth or using immersion optics, spherical aberrations and self-focusing are negligible. The threshold for multiphoton ionization is then met at the geometrical focus, where the excited electron density will dramatically increase due to impact ionization. Since the ionization is confined to a small volume, the energy is quickly transferred to the lattice producing a pressure which subsequently drives a shock wave and stress that exceeds the Young modulus of the material. A micro-explosion occurs at the focus and results in the formation of a void as small as 200 nm within a compressed shell [12–14].

If the input pulse exceeds the critical power or focuses at a deeper depth in the bulk of a material, the energy is deposited over a larger volume around the focus instead of converging at a point leading to the formation of void arrays [15]. Spherical aberration can further expand

the energy deposition region resulting in an elongated plasma channel. After plasma rapidly transfers energy to the lattice, a cylindrical shock wave emerges leading to the rupture of the material behind the wave's crest. The formation of such channels by single pulse irradiation have been previously observed, which would then break into chains of voids by subsequent irradiation [16]. Meanwhile single pulse imprinting of void arrays have been reported [17]. Other studies suggest void arrays arise from the interference of ultrafast laser driven electron waves interfering to create a standing electron plasma wave, inducing multiple periodic microexplosions [18]. However, in all of these studies, it is unsure that critical electron densitys are met. Regardless of the mechanism, optical cavitation in glass can lead to type III modification in the irradiated zone [19]. The above classification of modification regimes has been regarded as a non-reversible path following the laser intensity regimes.

Currently, the formation mechanism for self-assembled nanogratings is still under debate. Therefore, an understanding of the environment during laser irradiation that facilitates nanograting formation is pivotal. While many different models have been proposed [7,8,20–27], there exists a few mainstream theories on the formation mechanism. When nanograting formation was first discovered, the periodicities were thought to be due to an interference of generated Langmuir waves from a critical plasma [7]. The other mainstream view describes the evolution of nanoplasma hot spots, which form inhomogeneously around defects and/or color centers [8,20]. This theory is also explained to be in an environment of high to critical plasma densities. To overcome the issue of critical plasma densities, the exciton-polariton model was introduced and also explained the longitudinal periodicity of nanogratings based on the interference of short-living exciton polaritons [22,23]. Only recently studies have tried to combine the different theories in order to use the same interference models to explain the periodicities. The nanoplasmonic model was further expressed on as an excitation of standing plasma waves at the interfaces of modified-unmodified regions [26]. This excitation at the interface leads to areas of critical plasma densities, promoting the generation of interfering Langmuir waves resulting in periodic nanogratings similar to the original interpretation as well as the mechanism thought to be responsible for surface ripples formation [26]. This theory was taken further suggesting the mechanism is based on the interference between incident waves from the laser source and scattered waves from random inhomogeneities [27]. This interference results into the organization of nanoplanes with wavelength-based periodicity dependent on the density of the inhomogeneities resulting in a dependence on the electron density. However within each of these theories, there are issues that invalidate the models such as dependencies on number of laser pulses and/or pulse energies with respect to periodicities, material dependencies and limitations on intensities and electron density. Therefore, the identification of the electron density during laser irradiation is crucial for the fundamental understanding of the formation mechanism.

Recently, it was observed that under moderate focusing conditions (NA > 0.4) in fused silica self-assembled nanogratings (type II) could be developed from void formation (type III) after the first few pulses [28]. While void formation is not necessary for the formation of nanogratings [28], it is interesting to observe type II modification after void formation when it was originally theorized that near-critical threshold plasma densities are met when the voids are visible [29,30]. In this paper, we studied the characteristics and evolution of femtosecond laser-induced structures in fused silica in a multi-pulse regime under tight focusing. The transition from voids to nanogratings was observed and compared against numerical simulations of the distribution of the laser fluence, incident intensity, and electron density of a single femtosecond pulse by solving the nonlinear Schrödinger equation. Here we discuss the possible role of pulse incubation effects in the structural modification. Understanding the role of energy absorption in the regimes of the void to nanograting transition can shed light on the dynamics for laser induced nanostructuring.

2. Experimental setup

A mode-locked, regenerative amplified Ti-sapphire laser system (Spitfire, Spectral Physics Ltd.) delivered 120 fs (FWHM) laser pulses with a repetition rate of 1 kHz at a centre wavelength of 800 nm (photon energy 1.55 eV). A Glan polarizer and a λ/2 waveplate were used to adjust the pulse energy and polarization azimuth angle, respectively. The laser beam was focused with a 50× objective (LU Plan, Nikon) (NA=0.55) into the bulk of commercial grade silica glass mounted onto a computer-controlled XYZ translation stage (H101A ProScan model, PSI). The beam waist at the focus was estimated to be 0.8 μm. The geometric focus was fixed at a depth of 150 μm with respect to the surface of the sample throughout all the experiments.

3. Results and discussion

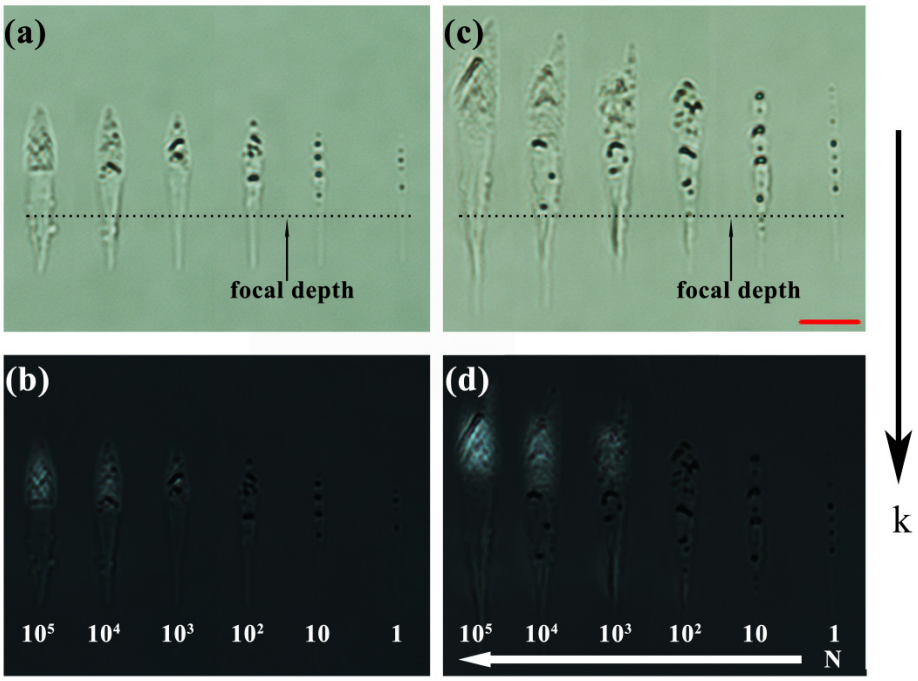

Fig. 1. (a) and (c) Optical images of the dependence of femtosecond laser-induced structures on the input pulse numbers. (b) and (d) Birefringence of the induced structures under cross-polarization illumination. E= 1 μJ (left column) and 2 μJ (right column). As the pulse number increases, the voids formed after the first few pulses transition to birefringence located at the top of the structure, as indicated under cross-polarizers. **k** represents the laser propagation direction, and the red bar is 10 μm.

A series of dots with increasing pulse number were imprinted in the bulk of fused silica (Fig. 1). The dependence of the induced structures on number of pulses was analysed with an optical microscope under two optical illumination modes, i.e., standard and cross-polarized. An elongated trace was observed stretching along the beam propagation direction and structural modification emerges before the geometrical focus. Alongside the observed contour changes of the induced structures, their evolution with respect to pulse number is also important. A chain of voids appears in the exposed area within the first 10 pulses. However, as the pulse number increases, the voids multiply and develop in both directions (towards top and bottom) and disperse in wide region. Finally, this leads to the emergence of an observable optical birefringence at the top of the induced structure as shown in Figs. 1(b) and 1(d). This

transition indicates that voids, which occur after a few initial pulses, gradually evolve into nanogratings.

The nanograting formation has been previously theorized being an accumulative process, which is sensitive to the density of defects from silica decomposition [31,32]. During multi-pulse irradiation, the presence of defects in the exposed area creates energy levels within the material band gap of silica and facilitates the production of free electrons that seed the impact ionization; the electron density will be enhanced by the successive input pulses. Consequently, distribution of induced defects or excited plasma depends not only on the number of pulses, but also on a series of factors associated with the spatial distribution of the incident energy. Therefore, we performed a theoretical study on the laser fluence, incident intensity and electron density around the focus.

For simulations we used the nonlinear Schrödinger equation for tightly focused femtosecond pulse propagation. The basis of the model is similar to a previous study in [33]:

$$\frac{\partial E}{\partial z}=\frac{i}{2k}\nabla_{\perp}E-\frac{ik''}{2}\frac{\partial^2 E}{\partial^2\zeta^2}-\frac{\sigma}{2}\left(1+i\omega\tau_c\right)\rho E-\frac{1}{2}\beta^{(m)}\left|E\right|^{2m-2}E+ik_0n_2\left|E\right|^2E \qquad (1)$$

where ζ refers to the retarded time variable t-z/v_g . The terms on the right-hand side of Eq. (1) respectively stand for the diffraction, group velocity dispersion (with coefficient $k''=361fs^2/cm$) [29], absorption and light defocusing of electron plasma, six-photon absorption (with coefficient $\beta^{(m)}=2.7\times10^{-65}cm^9/W^5$) [34], as well as Kerr self-focusing ($n_2=2.5\times10^{-16}cm^2/W$) [35].

The electron density involved in Eq. (1) can be further quantified by the following rate equation:

$$\frac{\partial\rho}{\partial t}=\frac{1}{n_0^2}\frac{\sigma}{E_g}\rho\left|E\right|^2+\frac{\beta^{(m)}}{m\hbar\omega}\left|E\right|^{2m}-\frac{\rho}{\tau_c} \qquad (2)$$

For fused silica at 800 nm, the linear refractive index $n_0=1.45$, and the absorption cross-section of inverse bremsstrahlung $\sigma=k\omega_0\tau_c/n_0^2\rho_c\left(1+\omega_0^2\tau_c^2\right)=1.55\times10^{-18}cm^2$ [36]. Here the electron scattering time is $\tau_c=23.3fs$ [29].

Since the refractive index mismatch between air and silica glass potentially plays a role in the laser intensity distribution near the focus of a high NA objective [37], we further incorporate the effect of the spherical aberration into the present model. For example, a relative complete set of the equations for the electric field distribution has been expressed by Török et al. [38]. In our simulation, the light field distribution in fused silica glass in the proximity of the interface, which was computed from Eq. (2), was chosen as the initial condition of the coupled Eqs. (1) and (2). The radial range of the simulation was chosen to be 20 times the waist of the incident light at the interface to make sure that no reflection comes from the boundary of the computational domain. Also, it has been noted that spherical aberration could be ignored if a laser pulse is focused by a lens with focal length of ~mm, even though a similar NLSE approach is used to simulate the fluence and plasma distribution in transparent materials [39]. Alternately, Couairon et al. also simulated numerically the intensity distribution at the focal point by using a pair of parabolic mirrors to overcome spherical aberration arising from the focusing geometry [40]. This approach offers an optional route to avoid the effect of spherical aberration on the induced microstructures.

Looking at the laser fluence and maximum intensity distribution for a single pulse during the pulser duration (Fig. 2), it is easy to see that the modification will take a tear-like shape structural distribution. The laser fluence sufficient to induce plasma can be seen well before the geometrical focus. As the input energy increases, the ionization onset is shifting farther from the geometrical focus.

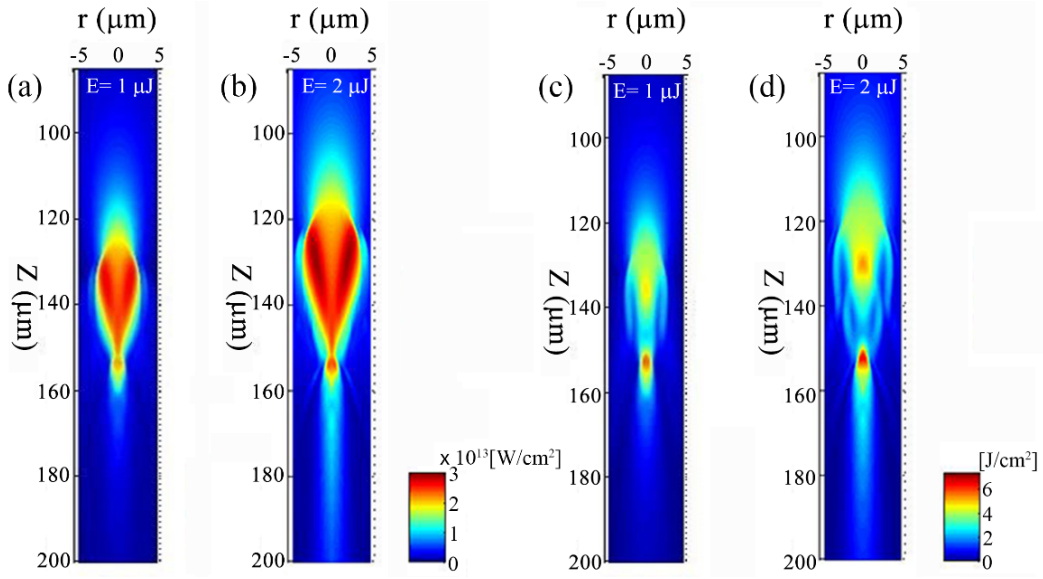

Fig. 2. (a) and (b) Maximum intensity and (c) and (d) laser fluence simulations for a single pulse at 1 and 2 μJ, respectively. Large tear-like distributions with modification occurring before the focus is seen, as observed in experiment. The laser-induced breakdown reaches as high as ~2.5×10^{13} W/cm^2 and the laser fluence is larger than the threshold for fused silica of 2-3 J/cm^2 (4.45 and 5.35 J/cm^2).

Another notable feature of the simulated profile is the on-axial spread of the generated field distribution along the beam propagation direction. This is due to the redistribution of the laser energy resulting from the mismatch of the refractive indices between air and glass, resulting in spherical aberration. Compared to the previous models without consideration of spherical aberration [29,36], a secondary focus emerges at the end of the profile because in a paraxial situation, the light at the laser beam edge can converge to a deeper depth. It is also worth noting that the local intensity and electronic excitation in other areas are relatively weak in contrast to what is observed before the geometrical focus. This implies that areas with less intensity, such as the long filament at the end of the entire structure, play a minimal role in structural change even under multi-pulse exposure.

The intensity threshold for femtosecond laser-induced breakdown and damage in fused silica is presumed to be 3.2×10^{13} W/cm^2 [41], which agrees with our simulations in which the peak intensities before the geometrical focus are respectively 2.4 and 2.49×10^{13} W/cm^2 for 1 and 2 μJ. In addition, fused silica breakdown threshold has been suggested at 3 J/cm^2 at 800 nm for a pulse duration of 10~100 fs [30] or at 1.87 J/cm^2 by an 800 nm laser pulse for 160 fs [42]. The two thresholds are below the maximum values of 4.45 and 5.35 J/cm^2 in our two cases.

The shape of permanent modification is mapped by calculating the electron density profile after single pulse exposure (Fig. 3). It can be clearly seen in the experimental results, that a single pulse results in a chain of voids. In the region where the voids are observed in the experiment, the electron density from the simulation ranges from 1.07 to 1.49×10^{20} cm^{-3} inside the 11 μm-long void formation area in the 1 μJ case, and 1.14 to 2.55×10^{20} cm^{-3} inside the 13 μm-long area in the 2 μJ case. Integrating over the entire structure shown in the numerical simulations approximated as an ellipsoid, we calculated that 10-20% of the pulse energy is absorbed. The simulation indicates that the electron density before the geometrical focus is ~10^{20} cm^{-3}, which is one order of magnitude lower than the critical threshold of 1.7×10^{21} cm^{-3} in fused silica. The simulation result alongside our experimental results indicates that at sufficient femtosecond pulse energies, the relatively large ionized area within an electron density >10^{20} cm^{-3} can facilitate void formation. For void formation to occur,

optical cavitation must occur in the glass. Optical cavitation can only occur if the energy deposited during irradiation exceeds the Young's Modulus of the material, regardless of the electron density present. For fused silica, the elastic modulus is roughly 73 GPa. Therefore, for a 1 μm^3 void, the energy deposited to induce the void is 0.073 μJ. Based on the total volume of the voids formed in a single pulse as seen in the experimental results (~1.362 μm^3 for 1 μJ and ~2.18 μm^3 for 2 μJ), roughly 8-10% of the pulse energy is deposited into the bulk for the formation of the voids, which agrees well with the calculated absorption from the electron density simulations.

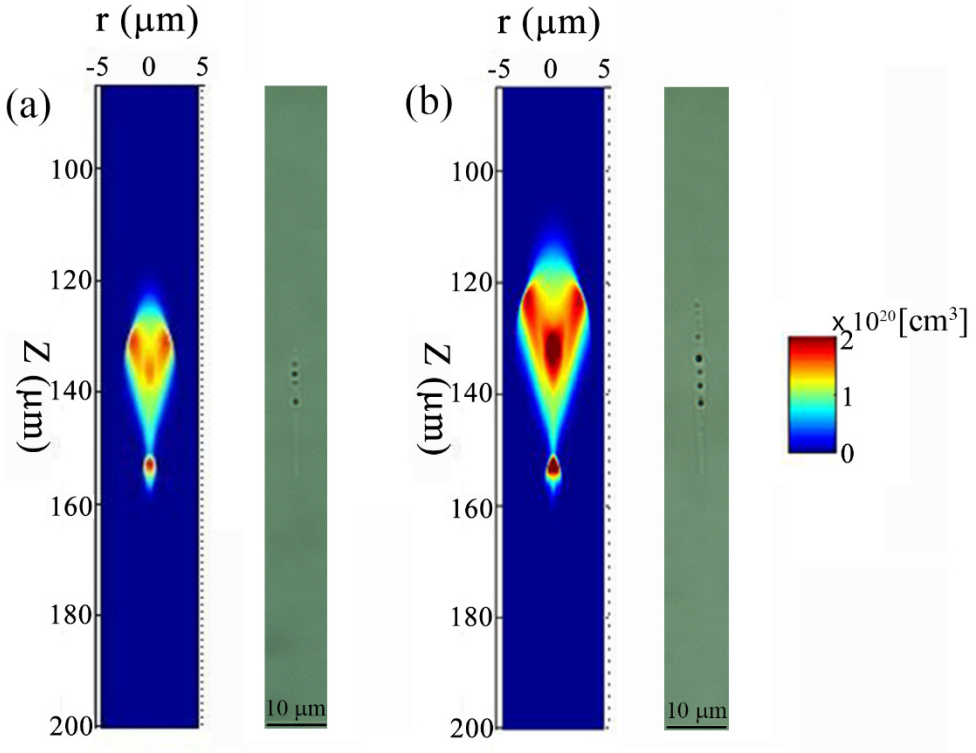

Fig. 3. Electron density simulation for single pulse irradiation for (a) 1 μJ and (b) 2 μJ alongside optical images of the experimental observation. In the regions where the electron density reaches above 10^{20} cm^{-3}, void formation is observed in the structures printed.

The pre-formed voids appearing in the exposed area act as additional scattering centres of light [16,28]. This scattering distorts the intensity distribution of the incident light, leading to a spatial redistribution of the femtosecond pulse energy. As a result, the formed voids multiply, merge and move towards the incident surface within tens of pulses in the areas of lower density or viscosity phase [16]. As more pulses arrive to the area of interaction, the incoming light can be scattered simultaneously with the expansion of the emerging plasma by an increase in local centers distributing in larger areas. Therefore the deposited energy will introduce local defects in the glass and accelerate the structural transition and rearrangement before the geometrical focus after further irradiation [43].

Meanwhile, the relatively strong electron-phonon coupling in fused silica leads to the formation of excitons. The excitons become self-trapped, driving local atomic deformations and displacements. Subsequently, the self-trapped excitons decay into E' centres together with non-bridging oxygen hole centres (NBOHC) on a time scale of 250 fs [31]. The NBOHC can react with E' centres when some critical density is reached forming oxygen deficiency centres (ODC(II)), which is observed simultaneously with the occurrence of nanogratings [31,32]. These defects lower the threshold for photon-ionization compared to that of pristine glass.

Following several studies, we estimate that electrons excited from defect states account for roughly 1-2% of the total electron density [44]. This introduces a circumstance for pulse incubation effects to bridge the time gap between two successive pulses in a continuous exposure no matter how long the pulse interval is [22,31].

With respect to the electron density, to reach the critical threshold, the glass needs to absorb 10 times more energy. Even assuming that 50% of the pulse is absorbed [36], it is insufficient to reach the critical electron density in the excited regions where void formation is seen. A growing number of evidence suggests that structural changes may take place in a phase of underdense plasma [29,36]. Pump probe experiments show that initial electron densitys as low as 10^{19} cm^{-3} is enough for inducing permanent restructuring in fused silica [45,46]. Low-spatial-frequency periodic structures on the surface of fused silica glass and nanogratings formed in high-silicate nanoporous glass have been reported to form at low degrees of material excitation (N_e~5×10^{20} cm^{-3}) based upon Drude formalisms used to simulate and confirm what is seen in experiment [25,26,47]. Since self-assembled nanogratings are observed after the void state at lower than critical threshold plasma densities, it is then concluded to be near impossible to reach the critical density threshold even with further irradiation.

The idea of lower than critical densitys has consequences with interference-based models where the spacing between the nanoplanes is dependent solely on the plasma temperature and electron density [7,23]. It also provides difficulty in explaining the electron densitys needed for standing plasma waves to be produced in the bulk from the interfaces of a nanoplasma when trying to unify the theories on in-volume nanogratings based on surface ripples with the nanoplasmonic model [26]. While local field enhancements in underdense nanoplasmas are known to be stronger than the incident field in an underdense plasma [48], it is still difficult to explain the order of magnitude increase in electron density to reach critical densitys as well as any sort of physical process taking place in such an environment. Therefore, we suggest that the formation mechanism of self-assembled nanogratings should take into account low electron density in future studies.

4. Conclusion

In summary, we have studied the structural transition from type III to type II in fused silica via a femtosecond laser pulse incubation effect. The void formation appears before the geometrical focus after the initial few pulses, and nanograting gradually forms at the top of the induced structure with subsequent irradiation. For comparison, a nonlinear Schrödinger equation considering the effect of spherical aberration is used to simulate the distribution of laser fluence, incident intensity and electron density in the laser pulse beam propagation. The simulations show that optical breakdown happens before the geometrical focus. This process leads to the formation of voids due to cavitation in the area where the electron density exceeds 10^{20} cm^{-3}. However, estimations based on energy absorption show that the exited electron density is insufficient to reach the critical threshold that was once assumed to occur in the regime of void formation and nanogratings. Our study provides experimental evidence to support the transition from the induced voids to nanograting and states the limitations, which may be useful to explore the potential formation mechanism of nanogratings.

Funding

This work is financially supported by the Engineering and Physical Sciences Research Council (EPSRC) (EP/M029042/1), China Scholarship Council (CSC) (201406895013), Shanghai University International Cooperation and Exchange Fund, National Natural Science Foundation of China (NSFC) (61205128), Shanghai Natural Science Foundation (SNSF) (13ZR1414800, 14ZR1415400).

Acknowledgments

The authors would like to thank Rokas Drevinskas for his input during our very fruitful discussions. All data in this paper was deposited into the University of Southampton Library Repository (DOI:10.5258/SOTON/385798)